


Equality scale-based and sound horizon-based analysis of the Hubble tension

Zhihuan Zhou^{✉,*}, Yuhao Mu, Gang Liu[✉], and Lixin Xu^{✉,†}

Institute of Theoretical Physics, School of Physics, Dalian University of Technology, Dalian 116024, People's Republic of China

Jianbo Lu[✉]

Department of Physics, Liaoning Normal University, Dalian 116029, People's Republic of China

 (Received 20 October 2022; accepted 10 March 2023; published 22 March 2023)

The Hubble horizon at matter-radiation equality (k_{eq}^{-1}) and the sound horizon at the last scattering surface [$r_s(z_*)$] provides an interesting consistency check for the standard Λ Cold Dark Matter (Λ CDM) model and its extensions. It is well known that the reduction of r_s can be compensated by the increase of H_0 , while the same is true for the standard rulers k_{eq} . Adding extra radiational component to the early Universe can reduce k_{eq} . The addition of early dark energy (EDE), however, tends to increase k_{eq} . We perform k_{eq} - and r_s -based analyses in both the EDE model and the Wess-Zumino dark radiation (WZDR) model. In the latter case, we find $\Delta H_0 = 0.4$ between the r_s - and k_{eq} -based datasets, while in the former case, we find $\Delta H_0 = 1.2$. This result suggests that the dark radiation scenario is more consistent in the fit of the two standard rulers (k_{eq} and r_s). As a forecast analyses, we fit the two models with a mock k_{eq} prior derived from *Planck* best-fit Λ CDM model. Compared with the best-fit H_0 in baseline Λ CDM model, we find $\Delta H_0 = 1.1$ for the WZDR model and $\Delta H_0 = -2.4$ for EDE model.

DOI: [10.1103/PhysRevD.107.063536](https://doi.org/10.1103/PhysRevD.107.063536)

I. INTRODUCTION

The Cepheid-calibrated supernovae Ia (SnIa) ($z \lesssim 1.6$) [1,2], the acoustic scale extracted from the cosmic microwave background (CMB) ($z \sim 1100$) and the baryon acoustic oscillations (BAOs) feature measured in large scale structure (LSS) surveys [3–6] ($z \sim 0.4$) are among the most precise cosmic distance anchors. Mismatches between these anchors give rise to the well-known H_0 discrepancy [7–9]. Specifically, the measured H_0 from the local distance ladder¹ is significantly higher than that inferred from the CMB [11,12] and BAO [4,13,14], and both of the latter two rely on the determination of the sound horizon scale at either the last scattering surface [$r_s(z_*)$] or the drag epoch [$r_s(z_d)$].

Direct solutions to the H_0 discrepancy from a theoretical point of view² can roughly be categorized as as the late-time ($z \lesssim 2$) [17–28] and the early-time

deformations [29–37]. Indirect solutions includes extending neutrino models [38,39], interacting dark sectorb [43,45–49], and other approaches [40–42,44,50–53]. The late solutions include a phantom transition of dark energy (DE), which raises the CMB predicted H_0 value while preserving the overall shape of the CMB spectra (including r_s) [21,24,25]; however, such modifications would violate the BAO predictions. To shift both the CMB and BAO anchors at the same time, one may consider reducing the sound scale at last scattering, $r_s(z_*)$ by adding extra component, e.g., early dark energy [30,34,35,54–57] and dark radiation [29,58–64]. In this case, the H_0 tension can still not be fully resolved [65,66]. One reason is that the additional component, e.g., early dark energy (EDE), would bring in new tension with the density fluctuation amplitude (σ_8 or S_8) [54]. Note that the H_0 tension and S_8 tension are unlikely to be independent [67–69]. Another is that, given a shift in r_s , the shift in H_0 needed to match CMB will be different from the one needed to match the LSS [70].

Historically, much of the focus has been put on r_s . To shed light on the H_0 discrepancy, additional standard rulers, especially those in the early Universe, are urgently needed. In this work, we focus on the standard ruler k_{eq}^{-1} , i.e., the Hubble horizon at matter-radiation equality, which can be derived from the turnover scale of the full shape (FS) power spectrum. The isolation of k_{eq} -based information in the FS

*11702005@mail.dlut.edu.cn

†lxxu@dlut.edu.cn

¹The local distance ladder depends on the choice of local calibrator, i.e., the Cepheid-calibrated SnIa from SHOES found $H_0 = 73.04 \pm 1.04$ [2], while $H_0 = 69.8 \pm 1.9$ [10] when the local distance ladder is calibrated by the tip of the red giant branch methods.

²It is possible that the H_0 tension is caused by unknown systematics. Many recent works focus on this issue [15–17].

galaxy power spectrum [71,72] (or CMB lensing power spectrum [73]) requires r_s -marginalization operations, which can be achieved either by excluding the prior on the baryon density ω_b [71] or removing the BAO features in the matter power spectrum via rescaling of the BAO wiggles [72]. It is shown in Ref. [74] that more information can be extracted from the features of FS power spectrum by adopting the latter approach. When combined with CMB lensing and Ω_m prior from the recent Pantheon + analysis [75], the standard ruler k_{eq} is able to deliver precise cosmological constraints. Especially, k_{eq} probes the features of new physics around the equality a_{eq} , which is otherwise difficult to detect.

The additional EDE component which peaked around the equality scale ($\log_{10} z_c \sim 3.5$) would increase the expansion rate $H_{\text{eq}} \equiv H(a_{\text{eq}})$ as well as the equality scale $k_{\text{eq}} \equiv a_{\text{eq}} H_{\text{eq}}$, while reducing the sound horizon scale $r_s(z_*)$. In mock EDE cosmology,³ one would notice a significant peak shift in H_0 measured from k_{eq} - to r_s -based analysis if the Λ CDM model were assumed [72]. This method provides a novel consistency check of the Λ CDM cosmology. On the other hand, the H_0 value measured by the two rulers should be consistent as long as the assumed model is correct. Thus, it is of particular interest to answer whether the modifications to the early Universe can shift both of the rulers (k_{eq}, r_s) so that the inferred H_0 from each of the rulers is consistent with late-time measurements. Note that the redshift of equality z_{eq} is sensitive to the change in the radiational (matter) component. An addition of a radiation component before the equality will reduce z_{eq} and thus shift k_{eq} to smaller value, which is in contrast with the shift brought by the extra DE component. Given k_{eq} (measured in unit of $h \text{ Mpc}^{-1}$) and a probe of Ω_m , one can solve for the Hubble constant [71]. We show in Sec. III that the reduction of k_{eq} will lead to a higher inferred value of H_0 compared with the best fit of the Λ CDM model.

One example of adding the radiational component is the recently investigated Wess-Zumino dark radiation (WZDR) model. The cosmological features of the WZDR model can be effectively described by a step transition of the effective number of neutrinos, N_{eff} , when the interacting dark radiation density increases as the mediator deposits its entropy into the lighter species. Compared with the reference self-interacting dark radiation model, the transition of radiation component in the WZDR model will shift the position of the high- ℓ modes, which enter the horizon before the step. It is shown in Ref. [58] that including such “stepped” dark radiation does significantly improve the combined fit to CMB, BAO, and SH0ES data while not degrading the fit to the CMB and BAO.

The outline of this paper is as follows. In Sec. II, we take a brief review of the basic equations associated with the

WZDR model. In Sec. III, we show how the EDE and WZDR models affect the standard ruler k_{eq} . In Sec. IV, we describe our numerical implementation of both models and the datasets used in our analysis. The numerical results of the Markov chain Monte Carlo (MCMC) analysis are presented in Sec. V. The discussion and conclusions are presented in Sec. VI.

II. MODELS

In this section, we present the basic features of the WZDR model [76] for cosmological implementations. We refer the reader to Appendix A in Ref. [58] for detailed discussions. The interacting dark radiation consists of a Weyl fermion ψ and complex scalar ϕ , which interact through a Yukawa coupling, $\lambda\psi^2\phi$. The Lagrangian reads

$$\mathcal{L}_{\text{WZ}} = \lambda\phi\psi^2 + \lambda^2(\phi^*\phi)^2. \quad (1)$$

This model is referred to as the “Wess-Zumino dark radiation. When the temperature of the coupled fluid drops below the scalar mass m_ϕ , the scalars deposit their entropy into the lighter (massless) ψ species. According to the entropy conservation, during this process, the lighter species would be heated, while the energy density of interacting fluid transitions as $N_{\text{wzdr}} \rightarrow N_{\text{wzdr,early}}$ at a redshift z_t , where

$$N_{\text{wzdr}} = \frac{\rho_{\text{wzdr}}}{\rho_{1\nu}} \quad (2)$$

is the effective number of WZDR in the present time, with $\rho_{1\nu}(a)$ the energy density of a single neutrino in standard Λ CDM cosmology. In the *Planck* best-fit WZDR model, the transition of N_{dr} happens just before the matter radiation equality, i.e, $\log_{10} z_t \approx 4.3 \pm 0.2$, which implies m_ϕ is of order of 1 or 10 eV. The fluid consists of both massive particle ϕ and massless particles ψ during the transition. After the transition, the massive particles ϕ have annihilated away so that the energy density of fluid in the present time is dominated by massless particle ψ , with

$$\rho_\psi = \frac{7}{4} \frac{\pi^2}{30} T_d^4 = \rho_{1\nu} f_T^4, \quad (3)$$

where $f_T \equiv T_\nu/T_{\text{dr}}$ is the temperature ratio between neutrinos and WZDR. Accordingly, the energy and pressure density of WZDR can be written as

$$\rho_{\text{wzdr}} \equiv \rho_\psi + \rho_\phi = \rho_{1\nu} [1 + r_g \hat{\rho}(x)] f_T^4 \quad (4a)$$

$$p_{\text{wzdr}} \equiv p_\psi + p_\phi = p_{1\nu} [1 + r_g \hat{p}(x)] f_T^4, \quad (4b)$$

where we have assumed

$$\rho_\phi = r_g \rho_\psi \hat{\rho}(x), \quad p_\phi = r_g p_\psi \hat{p}(x), \quad (5)$$

with $x \equiv m_\phi/T_{\text{dr}}$, and $r_g = 8/7$ is the density ratio of bosons to fermions for a single degree of freedom. Note that

³Euclid-like mock data are generated assuming the EDE model. See Ref. [72] for detailed discussions.

the dimensionless integrals $\hat{\rho}$ and \hat{p} can analytically be expressed in terms of the Bessel functions of the second kind. According to the entropy conservation in the dark fluid,

$$S \propto a^3 \frac{\rho_{\text{dr}} + P_{\text{dr}}}{T_{\text{dr}}} = \frac{\rho_{\text{dr},0} + P_{\text{dr},0}}{T_{\text{dr},0}}, \quad (6)$$

with $\rho_{\text{dr},0} = 3P_{\text{dr},0} = N_{\text{dr},0}\rho_{1\nu,0}$. Combing Eqs. (3), (4a), (4b), and (6), one can solve $x(a)$ numerically, while f_T can be expressed in terms of $x(a)$, i.e., can be expressed as

$$f_T = f_{T,0} \frac{a}{xa_t} = f_{T,0} \left(1 + \frac{r_g}{4} [3\hat{\rho}(x) + \hat{p}(x)] \right)^{-1/3}, \quad (7)$$

where $f_{T,0} = N_{\text{dr},0}^{\frac{1}{4}}$ and $a_t \equiv T_{\text{dr},0}/m_\phi$ is the transition scale factor.

In this work, we assume one massive neutrino species with a mass of 0.06 eV and N_{ur} to be the effective number of ultrarelativistic (massless neutrino) species. We use the fractional contribution of WZDR to total ultrarelativistic species,

$$f_{\text{wzdr}} \equiv \frac{N_{\text{wzdr}}}{N_{\text{wzdr}} + N_{\text{ur}}}, \quad (8)$$

to parametrize the WZDR model [denoted as (f)WZDR]. Note that the EDE model can be parametrized by the maximal fractional contribution of the EDE component to the energy density of the universe, $f_{\text{EDE}} \equiv \rho_{\text{EDE}}(z_c)/\rho_{\text{tot}}(z_c)$ and the critical redshift z_c . As can be seen the (f)WZDR parametrization is analogous to the parametrization in EDE model. The WZDR model can also be effectively described by the effective number of additional neutrino species N_{wzdr} (equivalent to N_{IR} in Ref. [58]). Note that WZDR belongs to self-interacting radiation. We also include the analysis of free-streaming (noninteracting) radiation as a contrast, in which case N_{eff} is set as a free parameter.⁴ See Appendix A for the cosmological constraints on each of the parametrizations described above.⁵

III. IMPACT ON STANDARD RULERS

In Λ CDM model, the equality scale (in unit of Mpc^{-1}) can simply be approximated as

$$k_{\text{eq}} = (2\Omega_m H_0^2 z_{\text{eq}})^{1/2}, \quad (9a)$$

$$z_{\text{eq}} = 2.5 \times 10^4 \Omega_m h^2 \Theta_{2.7}^{-4} \quad (9b)$$

⁴Throughout this paper, we assume one massive neutrino species $N_{\text{ncdm}} = 1$. In this case, one can set either N_{eff} or N_{ur} to be a free parameter.

⁵ N_{ur} can either be a free parameter or be fixed at given value. In (f)WZDR parametrization, we find $N_{\text{ur}} = 2.00 \pm 0.27$, which closely matches the value given in standard cosmology. Consequently, we have fixed N_{ur} to 2.0328 in the following analysis.

with Ω_m the matter density fraction and $\Theta_{2.7} \equiv T_{\text{CMB}}/(2.7\text{K})$ the CMB photon temperature. The addition of the DE component in the early time does not change the ratio between matter and radiation. Thus, Eq. (9b) still holds in the EDE model (see the middle panel of Fig. 1). However, Eq. (9a) is no longer valid in this scenario because the extra energy component increases the expansion rate $H(z_{\text{eq}})$ while reducing the comoving horizon at equality scale (k_{eq}^{-1}). On the contrary, Eq. (9a) is valid in the WZDR scenario, whereas Eq. (9b) is not. The additional radiation component N_{wzdr} shifts z_{eq} to a smaller value, and k_{eq} is reduced as a consequence. As shown in

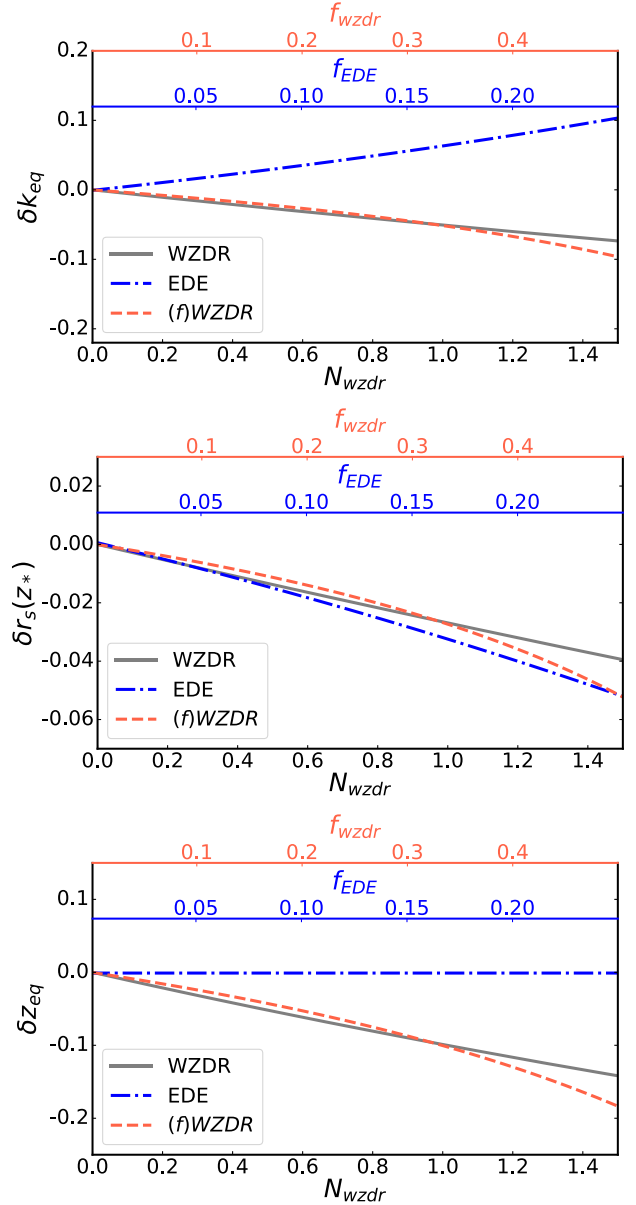


FIG. 1. The relative difference between the best-fit parameters (k_{eq} , r_s , z_{eq}) calculated in fiducial Λ CDM model and its extensions (EDE and WZDR).

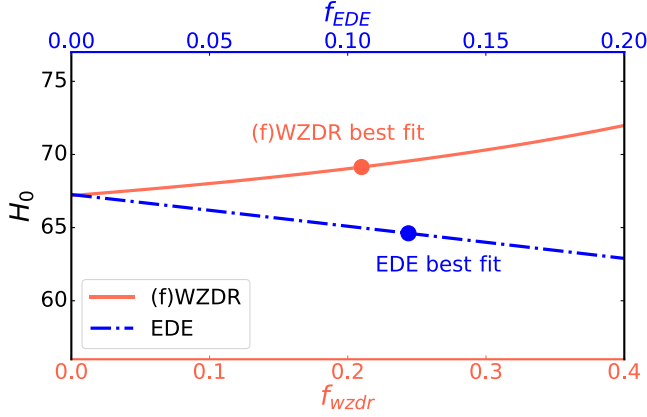


FIG. 2. The derived H_0 in EDE and (f)WZDR scenarios with k_{eq} and Ω_m fixed at *Planck* best-fit value assuming Λ CDM model.

Fig. 1, the addition of EDE and WZDR shifts the standard ruler k_{eq} differently, while the sound horizon $r_s(z_*)$ is reduced in both scenarios, which increases the inferred value of H_0 in r_s -based analysis.

H_0 is constrained by measuring the angular scale of the cosmological horizon at matter-radiation equality, i.e., $k_{\text{eq}}/D_A(z) \propto k_{\text{eq}}/h$ [74], which is equivalent to the value of k_{eq} in the unit of $h \text{ Mpc}^{-1}$ (if not stated otherwise, k_{eq} discussed in this paper is in the unit of $h \text{ Mpc}^{-1}$). As can be seen in Eqs. (9a) and (9b), given k_{eq} and a probe of Ω_m , one can solve for the Hubble constant [71]. We have discussed how different models shift standard ruler k_{eq} compared with the fiducial Λ CDM model. Next, we fix k_{eq} and Ω_m to the value inferred in *Planck* best-fit Λ CDM model,⁶ i.e., $k_{\text{eq}} = 1.545 h \text{ Mpc}^{-1}$, $\Omega_m = 0.311$, to see the best fit of H_0 in these scenarios by “shooting” the targeted k_{eq} value. We show in Fig. 2 the best-fit H_0 value as a function of the fractional density of EDE and WZDR. As can be seen, the increase of k_{eq} by EDE component can be compensated by a lower inferred value of H_0 , while the decrease of k_{eq} is compensated by a higher inferred value of H_0 . We will further verify this point by adopting a mock prior on k_{eq} in MCMC analysis (See Sec. V B).

The equality scale k_{eq} corresponds to the turnover scale of the matter power spectrum. Thus, the difference in k_{eq} between the two models can be reflected in the shape difference in the linear matter power spectrum. A distinctive phase shift between the spectra in the EDE model and WZDR model can be noticed in Fig. 3, which corresponds to different turnover scales in the two models (marked in vertical lines).

⁶The baseline Λ CDM cosmology $\{h = 0.6821, \omega_c = 0.1177, \omega_b = 0.02253\}$. We refer the readers to Sec. III A in Ref. [72] for detailed discussions.

IV. DATASETS AND NUMERICAL METHOD

Following Ref. [74], we consider the following combination as our base datasets (denoted as \mathcal{B}), which includes:

- (i) *Supernovae (SNe)*.—The derived k_{eq}/h (in unit of Mpc^{-1}) is degenerate with the matter density, i.e., $k_{\text{eq}}/h \propto \Omega_m^{1/2} h$ [see Eqs. (9a) and (9b)]; thus, the additional priors on Ω_m can improve the constraints on H_0 from the equality scale. We consider the Gaussian prior $\Omega_m = 0.338 \pm 0.018$ from the most recent Pantheon analysis [61].
- (ii) *Big bang nucleosynthesis (BBN)*.—Including the ω_b prior from BBN breaks the $H_0 - \omega_b$ degeneracy and will strengthen the sources of H_0 information from the equality scale. Consequently, a prior on the physical baryon density $\omega_b = 0.02268 \pm 0.00036$ is imposed to maximize the extracted information, following Ref. [28].
- (iii) *Spectral index and primordial amplitude*.—Following from previous works [41], we add a flattened Gaussian prior on A_s and n_s centred at *Planck* best fit [11] i.e., $n_s = 0.965 \pm 0.02$ and $A_s = (2.11 \pm 0.108) \times 10^{-9}$.

The base datasets \mathcal{B} can optionally be combined with:

- (i) *Galaxy power spectra*.—We adopt the method described in Ref. [72] to marginalize over r_s information in the galaxy power spectrum. This method can be applied to the current version of the BOSS DR12 galaxy survey dataset [77], which is part of SDSS-III [78,79]. These data split across two redshift bins (at $z = 0.38, 0.61$) in each of the northern and southern galactic caps. Following from previous work, we utilize the CLASS-PT implementation [80] with publicly available likelihoods,⁷ in which the power spectrum is modeled with the Effective Field Theory of large scale structure [81] including one-loop perturbation theory.
- (ii) *Baryon acoustic oscillation*.—measurements of the BAO signal at $z = 0.38, 0.51, \text{ and } 0.61$ from the BOSS DR12 galaxy power spectrum [4].
- (iii) S_8 prior.—We adopt the prior $S_8 = 0.800 \pm 0.029$ from KiDS-450 + GAMA [82]; similar results can be found in the measurement from the first-year data of HSC SSP20, for which $S_8 = 0.804 \pm 0.032$ [83].

We are interested in how the extra radiation (DE) component affects the Hubble constant inferred from the standard ruler k_{eq} . Hence, throughout the analysis, we fix the fractional density of additional components to the best-fit value obtained in cosmological analysis [see Appendix A for a detailed discussion of the best-fit

⁷Available at https://github.com/oliverphilcox/full_shape_likelihoods.

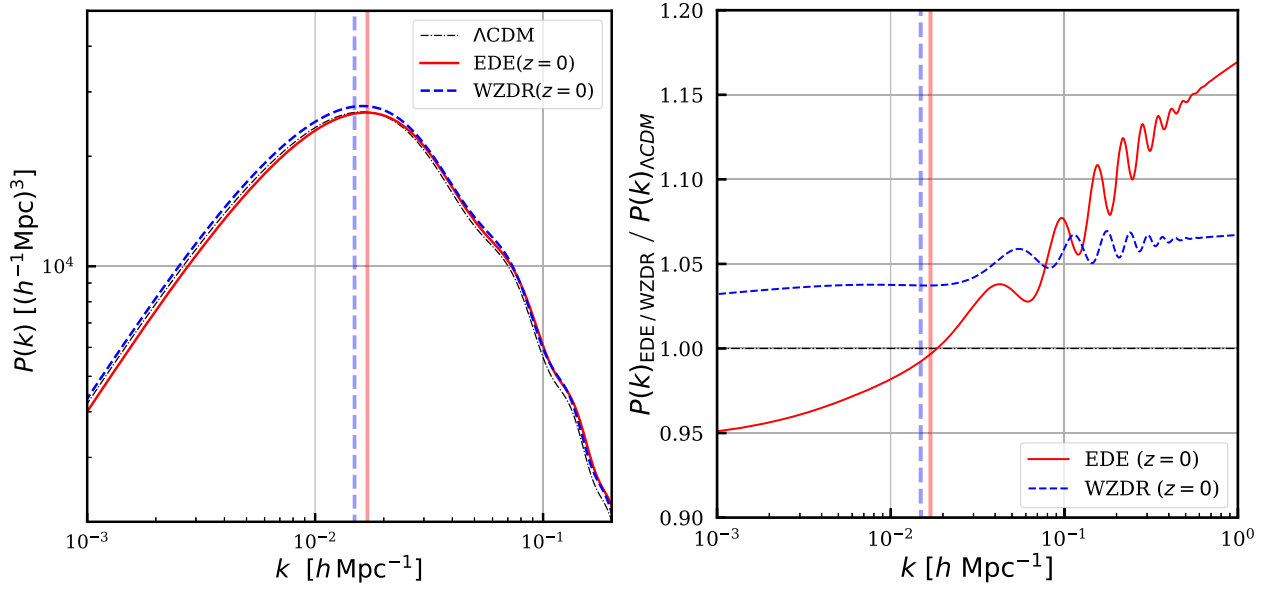


FIG. 3. Matter power spectra (left panel) and the ratio of spectra (right panel) at $z = 0$, for the *Planck* + FS best-fit EDE model and WZDR model with parameters given Table II. The fiducial Λ CDM model is set to the *Planck* 2018 best-fit parameters. The dashed and solid vertical lines correspond to the best-fit k_{eq} in the WZDR and EDE models, respectively.

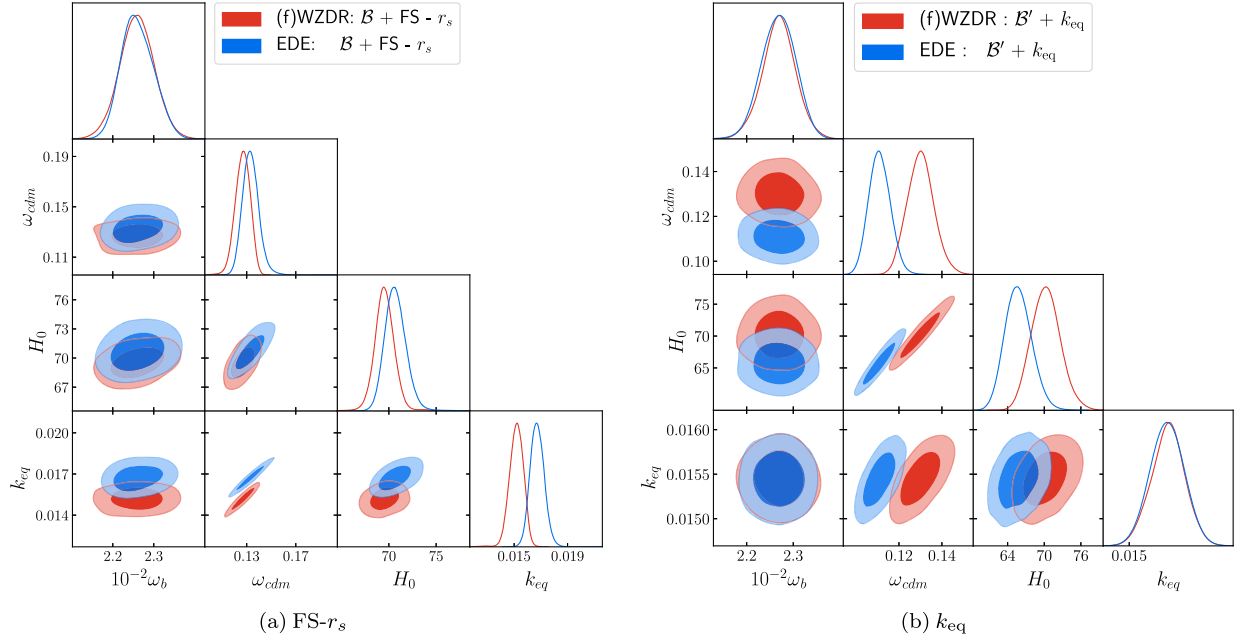


FIG. 4. Cosmological parameters constraints for EDE model (blue contour) and (f)WZDR model (red contour) from the dataset: $\mathcal{B} + \text{FS}$ power spectrum with r_s marginalized over (denoting as $\text{FS}-r_s$ in the left panel) and fitting to $\mathcal{B}' + k_{\text{eq}}$ prior derived from *Planck* best-fit Λ CDM model (right panel).

(f)WZDR model], i.e., $f_{\text{wzdr}} = 0.21$ and $f_{\text{EDE}} = 0.122$.⁸ We sample over the following set of cosmological parameters:

$$\{H_0, \omega_b, \omega_{\text{cdm}}, \log 10^{10} A_s, n_s, \sum m_\nu\}. \quad (10)$$

⁸We adopt the best-fit values of EDE model from Table I of Ref. [31].

The optical depth of reionization, τ_{reio} , is fixed to 0.055. We implement the EDE and the WZDR scenarios as modifications to the publicly available Einstein-Boltzmann code CLASS [84,85] package. The nonlinear matter power

spectrum required by redshift-space distortion likelihoods are computed using the `HMCODE` [86–88] implemented in `CLASS`. The MCMC analyses are performed using the publicly available code `MONTEPYTHON` [89].

V. NUMERICAL RESULTS

We show in the left panel of Fig. 4 and Table I the r_s -independent constraints from FS galaxy power spectra, supplemented by the base datasets \mathcal{B} which include priors on Ω_m from `PANTHEON+` and ω_b from `BBN`.

For comparison between constraints with and without r_s information, we show in Table II the parameter constraints obtained from four choices of likelihoods: (i), the FS likelihoods with r_s marginalized over, (ii) the FS likelihoods including the BAO information, (iii) the BAO likelihoods combined with S_8 prior derived from lensing experiments, (iv) the FS likelihoods combined with *Planck* 2018 low- ℓ TT+EE and high- ℓ TT+TE+EE power spectrum (Note that the each of the former three choices of likelihoods is combined with the base datasets \mathcal{B}). The triangular plot with the one-dimensional posterior

distributions and the two-dimensional contour plots for the constrained parameters are shown in Figs. 5 and 6. Meanwhile, we did the same analysis for free-streaming radiations (FSDRs) to see whether or not the shifts on the two standard rulers depended on radiation self-interactions (see Appendix B).

A. Derived equality scale

In the discussion of Sec. III, we have shown that the addition of the WZDR reduces k_{eq} while the opposite is true for the EDE component. As shown in Table II, the 1σ constraint of k_{eq} from r_s -based analysis (BAO + S_8) in the (f)WZDR model, $k_{\text{eq}} = 1.512 \pm 0.041$, is 2.4σ lower than that in the EDE model, $k_{\text{eq}} = 1.659 \pm 0.045$. Still, there is a 2.2σ tension between the EDE and (f)WZDR best-fit k_{eq} when fitting with the k_{eq} -based analysis (r_s -marginalized FS power spectra), while in each model, k_{eq} derived from the BAO + S_8 prior is close to that from the r_s -marginalized FS power spectrum. These results suggest that k_{eq} cannot yet be tightly (model-independently)

TABLE I. The mean $\pm 1\sigma$ constraints on the derived parameters in EDE and fWZDR model, as inferred from base datasets \mathcal{B} + FS power spectrum with r_s marginalized over (left panel), and the $\mathcal{B}' + k_{\text{eq}}$ prior derived from the *Planck* best fit. Upper and lower bounds correspond to the 68% C.L. interval.

Dataset Model	FS without r_s		k_{eq} prior	
	(f)WZDR	EDE	(f)WZDR	EDE
H_0	69.7 ± 1.1	70.6 ± 1.0	70.3 ± 2.4	$65.8^{+2.0}_{-2.3}$
$10^2 k_{\text{eq}}$	$1.517^{+0.055}_{-0.050}$	$1.673^{+0.048}_{-0.055}$	1.545 ± 0.020	1.545 ± 0.021
σ_8	0.809 ± 0.027	$0.820^{+0.025}_{-0.029}$	0.825 ± 0.035	$0.725^{+0.026}_{-0.030}$
Ω_m	$0.310^{+0.011}_{-0.0094}$	0.3129 ± 0.0088	$0.310^{+0.011}_{-0.0094}$	0.3129 ± 0.0088
χ^2_{min}	1072.06	1073.42	0.06	0.08

TABLE II. The mean and $1-\sigma$ constraints on cosmological parameters in the (f)WZDR model (top panel) from four choices of likelihoods: (i), the FS likelihoods with r_s marginalized over, (ii) the FS likelihoods including the BAO information, (iii) the BAO likelihoods combined with S_8 prior derived from lensing experiments, (iv) the FS likelihoods combined with *Planck* 2018 low- ℓ TT+EE and high- ℓ TT+TE+EE power spectrum (Note that the each of the former three choices of likelihoods is combined with the base datasets \mathcal{B}). Upper and lower bounds correspond to the 68% C.L. interval.

Model	Dataset	H_0	$10^2 k_{\text{eq}}$	σ_8	Ω_m	$\ln 10^{10} A_s$	n_s	χ^2_{min}
(f)WZDR	$\mathcal{B} + \text{FS} - r_s$	69.7 ± 1.1	$1.517^{+0.055}_{-0.050}$	0.809 ± 0.027	$0.310^{+0.011}_{-0.0094}$	$3.024^{+0.039}_{-0.031}$	0.973 ± 0.019	1072.06
	$\mathcal{B} + \text{FS}$	$69.90^{+0.90}_{-0.79}$	$1.515^{+0.047}_{-0.029}$	$0.817^{+0.020}_{-0.016}$	$0.308^{+0.011}_{-0.0042}$	$3.036^{+0.023}_{-0.034}$	$0.971^{+0.021}_{-0.026}$	1072.26
	$\mathcal{B} + \text{BAO} + S_8$	70.13 ± 0.96	1.512 ± 0.041	$0.813^{+0.019}_{-0.021}$	0.3042 ± 0.0082	3.1146 ± 0.0070	$0.9730^{+0.0037}_{-0.0032}$	2802.5
	<i>Planck</i> + FS	$71.00^{+0.44}_{-0.49}$	$1.489^{+0.011}_{-0.0099}$	$0.8430^{+0.0036}_{-0.0042}$	0.3064 ± 0.0022	3.037 ± 0.033	$0.963^{+0.016}_{-0.022}$	2869.8
EDE	$\mathcal{B} + \text{FS} - r_s$	70.6 ± 1.0	$1.673^{+0.048}_{-0.055}$	$0.820^{+0.025}_{-0.029}$	0.3129 ± 0.0088	3.030 ± 0.036	0.975 ± 0.020	1073.42
	$\mathcal{B} + \text{FS}$	71.6 ± 0.9	$1.692^{+0.053}_{-0.044}$	0.820 ± 0.023	0.3134 ± 0.0085	$3.000^{+0.035}_{-0.042}$	$0.969^{+0.018}_{-0.020}$	1073.58
	$\mathcal{B} + \text{BAO} + S_8$	71.8 ± 1.1	1.659 ± 0.045	0.819 ± 0.022	$0.3043^{+0.0076}_{-0.0091}$	3.032 ± 0.040	$0.964^{+0.015}_{-0.020}$	8.18
	<i>Planck</i> + FS	$70.80^{+0.53}_{-0.60}$	$1.6954^{+0.0071}_{-0.0062}$	$0.8668^{+0.0056}_{-0.0039}$	3.142 ± 0.0080	$3.136^{+0.012}_{-0.0083}$	0.9735 ± 0.0042	7.78

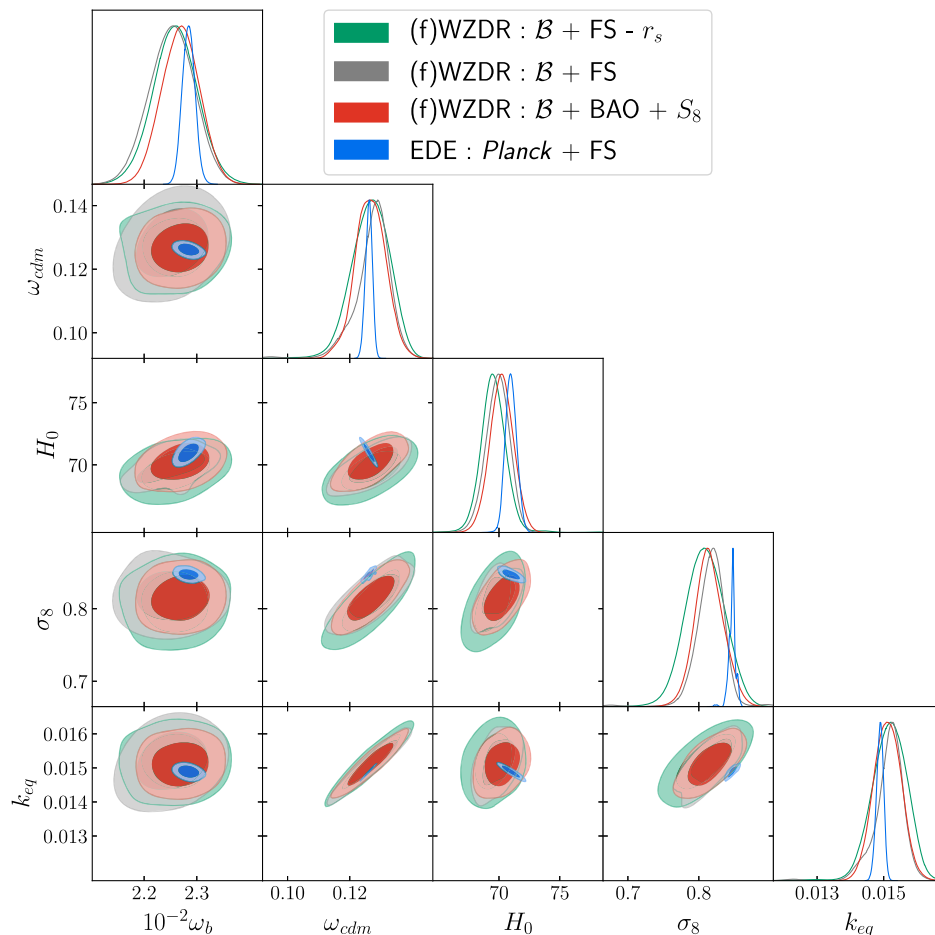


FIG. 5. Constraints on cosmological parameters in the WZDR scenario from four choices of likelihoods: (i), the FS likelihoods with r_s marginalized over, (ii) the FS likelihoods including the BAO information, (iii) the BAO likelihoods combined with S_8 prior derived from lensing experiments, (iv) the FS likelihoods combined with *Planck* 2018 low- ℓ TT+EE and high- ℓ TT+TE+EE power spectrum (Note that the each of the former three choices of likelihoods is combined with the base datasets \mathcal{B}).

constrained by the equality-based measurements. Currently, the information extracted from the r_s -marginalized FS power spectrum is dominated by information concerning structure growth ($f\sigma_8$, S_8) rather than the angular scale of the cosmological horizon at matter-radiation equality. Otherwise, the derived k_{eq} in k_{eq} -based analysis from different models should be more consistent.

B. k_{eq} - and r_s -based inference of H_0

In the WZDR model, we find a minor peak shift of $\Delta H_0 = 0.2$ between the fit of FS power spectrum with and without r_s information and a peak shift of $\Delta H_0 = 0.4$ from the k_{eq} - to r_s -based analyses (see Table II), while in the EDE model we have $\Delta H_0 = 1.0$ between FS and FS— r_s and $\Delta H_0 = 1.2$ between k_{eq} - and r_s -based analyses. Since the addition of radiation component shifts the two standard rulers more coherently (see the discussion

in Sec. III), the best-fit H_0 from r_s - and k_{eq} -based analyses in the WZDR model are more consistent than that in the EDE model. However, the above results are inconclusive since the Hubble constant measured by the two rulers is consistent (within 2σ) for both EDE and WZDR models. As is discussed above, k_{eq} -based datasets are dominated by the information $f\sigma_8$ (S_8) rather than the angular scale of the cosmological horizon at matter-radiation equality, which makes it difficult for us to detect the inconsistency.

To see how the standard ruler k_{eq} affects the inference of H_0 , we replace the r_s -marginalized FS power spectra with a mock prior: $k_{\text{eq}} = 1.545 \pm 0.020 \times 10^{-2} h \text{ Mpc}^{-1}$ derived from the *Planck* best-fit ΛCDM model (accordingly, the Ω_m prior in the supplement datasets \mathcal{B} are substituted by the *Planck* best-fit value, Ω_m , denoted as \mathcal{B}'). The results can be found in the right panel of both Table I and Fig. 4. As is discussed in Sec. III, to fit with the standard rulers fixed by

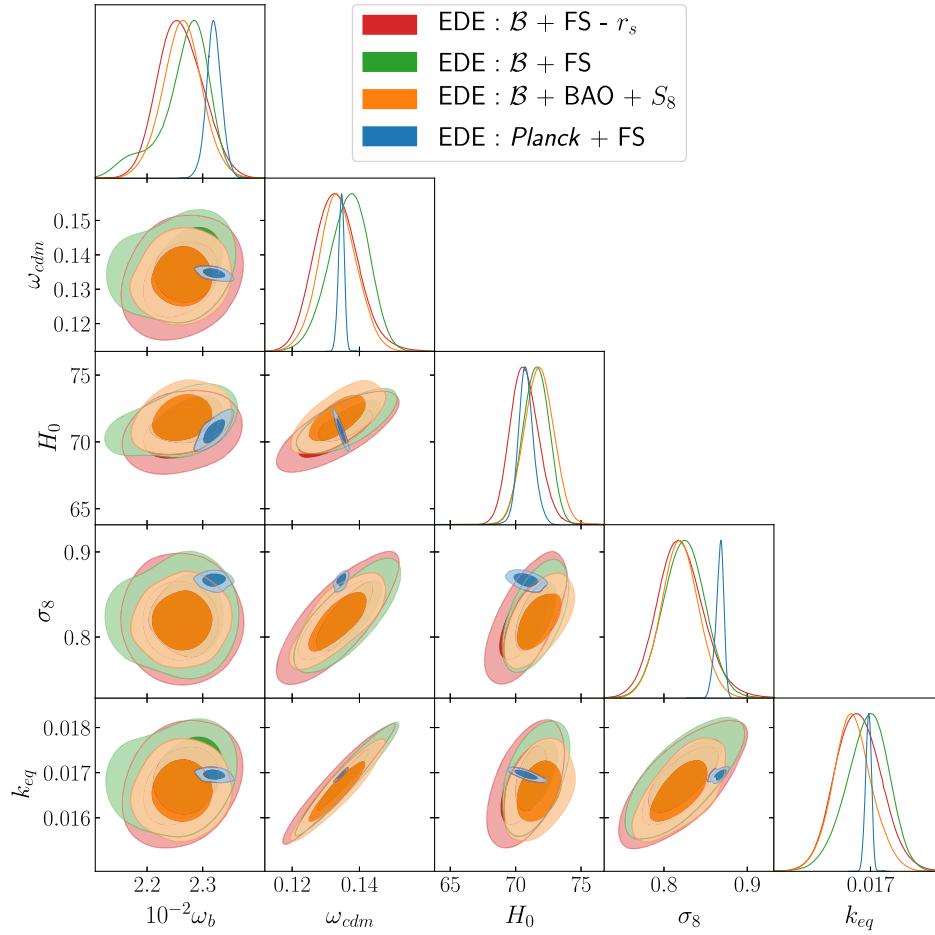


FIG. 6. Constraints on cosmological parameters in the EDE scenario from four choices of likelihoods: (i), the FS likelihoods with r_s marginalized over, (ii) the FS likelihoods including the BAO information, (iii) the BAO likelihoods combined with S_8 prior derived from lensing experiments, (iv) the FS likelihoods combined with *Planck* 2018 low- ℓ TT+EE and high- ℓ TT+TE+EE power spectrum (Note that the each of the former three choices of likelihoods is combined with the base datasets \mathcal{B}).

the fiducial Λ CDM model, the increase of k_{eq} should be compensated by a lower H_0 . Accordingly, its decrease should be compensated by a higher H_0 . In this case, the inferred value of H_0 in the WZDR model is significantly higher than in the EDE model. Note that we have also adopted a tight prior on Ω_m , so higher H_0 will result in higher $\omega_c = \Omega_m h^2 - \omega_b$ and higher σ_8 . The inferred σ_8 in the EDE model is much less than that of the WZDR model.

VI. CONCLUSIONS

The Hubble horizon at matter-radiation equality, k_{eq}^{-1} , provides valuable test of new physics around (prior to) z_{eq} , while the commonly used standard ruler, r_s , is sensitive to physics prior to the last scattering. These two rulers provide an interesting consistency check for the Λ CDM model and its extensions; i.e., the inferred value of H_0 from both the rulers should be consistent. We find that the addition of EDE component which peaked around the equality scale ($\log_{10} z_c \sim 3.5$) increases equality scale, k_{eq} . On the

contrary, the addition of a radiational component before the equality reduces z_{eq} and k_{eq} . We show in Fig. 2 that the increase of k_{eq} by EDE component can be compensated by an upward shift of H_0 , while the decrease of k_{eq} is compensated by a higher inferred value of H_0 . The two standard rulers should be shifted coherently to relieve the H_0 discrepancy between the early and late Universe.

Our numerical results shows that the best-fit H_0 values obtained from r_s - and k_{eq} -based analyses are consistent within 1σ in (f)WZDR model ($\Delta H_0 = 0.4$). In the same analysis assuming the EDE model, we observed a peak shift of $\Delta H_0 = 1.2$. There is significant tension between the derived k_{eq} in EDE and the (f)WZDR model. Meanwhile, in each model, k_{eq} derived from the BAO + S_8 prior is close to that from the r_s -marginalized FS power spectrum.

We have witnessed much tighter constraints on cosmological parameters when the FS power spectrum is combined by *Planck* 2018 datasets. The inclusion of *Planck* 2018 datasets has little impact on the best-fit value of H_0

and k_{eq} , while significantly increasing the density fluctuation amplitude σ_8 (see Table II). Meanwhile, the tension between derived k_{eq} in the (f)WZDR model EDE has increased from $\sim 2.5\sigma$ to $\sim 15\sigma$, owing to much tighter constraints from *Planck* datasets.

We expect more information on k_{eq} to be extracted from next generation of galaxy surveys, e.g., Euclid and SKA. As a forecast analysis, we adopt a mock prior derived from *Planck* best-fit Λ CDM model to see how the standard ruler k_{eq} affects the inference of H_0 . In the WZDR model, we find $\Delta H_0 = 1.1$ compared with the best-fit H_0 in the baseline Λ CDM model, while in the EDE model, the pair difference is $\Delta H_0 = -2.4$. This result further suggests that the two standard rulers should be reduced simultaneously to relieve the tension with the local distance ladder.

ACKNOWLEDGMENTS

This work is supported in part by National Natural Science Foundation of China under Grants No. 12075042, No. 11675032, and No. 12175095 (People's Republic of China) and by LiaoNing Revitalization Talents Program (Grant No. XLYC2007047).

APPENDIX A: BEST-FIT WZDR AND FSDR

We repeat the cosmological constraints on the WZDR model and FSDR model with the same datasets discussed in Ref. [90]. Meanwhile, we adopt a new parametrization with N_{ur} being a free parameter [denoted as (f)WZDR]. This dataset includes the *Planck* 2018 low- ℓ TT + EE and high- ℓ TT + TE + EE temperature and polarization power spectrum [11,91] as well as CMB lensing [11],

the BAO measurements [4,92,93], the PANTHEON supernovae data [94], and measurements from SH0ES [2] via a prior on the intrinsic magnitude of supernovae M_b [95]. Constraints at 68% C.L. (confidence limits) on the cosmological parameters and χ^2 statistics can be found in Table III. The posterior distributions and for WZDR, FSDR, and (f)WZDR parametrization are shown in Figs. 7, 8, and 9, respectively.

APPENDIX B: COMPARISON BETWEEN WZDR AND FSDR

For the constraint results shown in Table III, we have fit the WZDR and FSDR model with the same datasets. The amount of extra self-interacting (WZDR) and free-streaming dark radiation are parametrized by N_{idr} and ΔN_{eff} (ΔN_{ur}) respectively. We find the best-fit value of WZDR ($N_{idr} = 0.55$) is approximately twice the amount of the best-fit FSDR, $\Delta N_{eff} = 0.28$. Meanwhile, the inferred σ_8 value in the FSDR model (0.8461 ± 0.0064) is 3σ higher than that in the WZDR model (0.8185 ± 0.0059), which may exacerbate the tension with LSS experiments.

To test whether the shift on the two standard rulers (k_{eq}, r_s) depends on radiation self-interactions, we fix the extra WZDR and FSDR to the same amount, i.e., $N_{ur} = N_{idr} = 0.55$. We fit both of the models to the k_{eq} - and r_s -based datasets, and the results are shown in Fig. 10 and Table IV. As can be seen, the inferred H_0 (θ_s) and k_{eq} values are consistent (within 0.5σ) between the two scenarios. Thus, no evidence supports that the radiation self-interactions influence the two standard rulers.

TABLE III. The mean $\pm 1\sigma$ constraints on the cosmological parameters and derived parameters in the WZDR and (f)WZDR models from the datasets discussed in Appendix A. Upper and lower bounds correspond to the 68% C.L. interval.

Parameter	WZDR	(f)WZDR	FSDR
$10^{-2}\omega_b$	2.286 ± 0.018	2.279 ± 0.016	$2.279^{+0.013}_{-0.014}$
ω_c	$0.1263^{+0.0041}_{-0.0033}$	$0.1256^{+0.0026}_{-0.0029}$	$0.1220^{+0.0021}_{-0.0025}$
$\ln 10^{10}A_s$	3.046 ± 0.014	$3.047^{+0.021}_{-0.018}$	3.1240 ± 0.0057
n_s	$0.9725^{+0.0036}_{-0.0040}$	$0.970^{+0.010}_{-0.0092}$	$0.9859^{+0.0044}_{-0.0056}$
τ_{reio}	$0.0585^{+0.0059}_{-0.0069}$	0.0600 ± 0.0073	0.590 ± 0.0067
N_{idr}	$0.55^{+0.26}_{-0.19}$
f_{wzdr}	...	$0.21^{+0.11}_{-0.13}$...
N_{ur}	(2.0328)	2.00 ± 0.27	$2.31^{+0.10}_{-0.16}$
$\log 10 z_t$	$4.26^{+0.18}_{-0.20}$	$4.29^{+0.16}_{-0.19}$...
H_0	$71.0^{+1.3}_{-0.87}$	70.68 ± 0.89	$70.61^{+0.65}_{-0.88}$
σ_8	0.8185 ± 0.0059	$0.818^{+0.011}_{-0.010}$	0.8461 ± 0.0064
N_{eff}	$3.47^{+0.20}_{-0.15}$	$3.43^{+0.14}_{-0.16}$	$3.32^{+0.10}_{-0.16}$

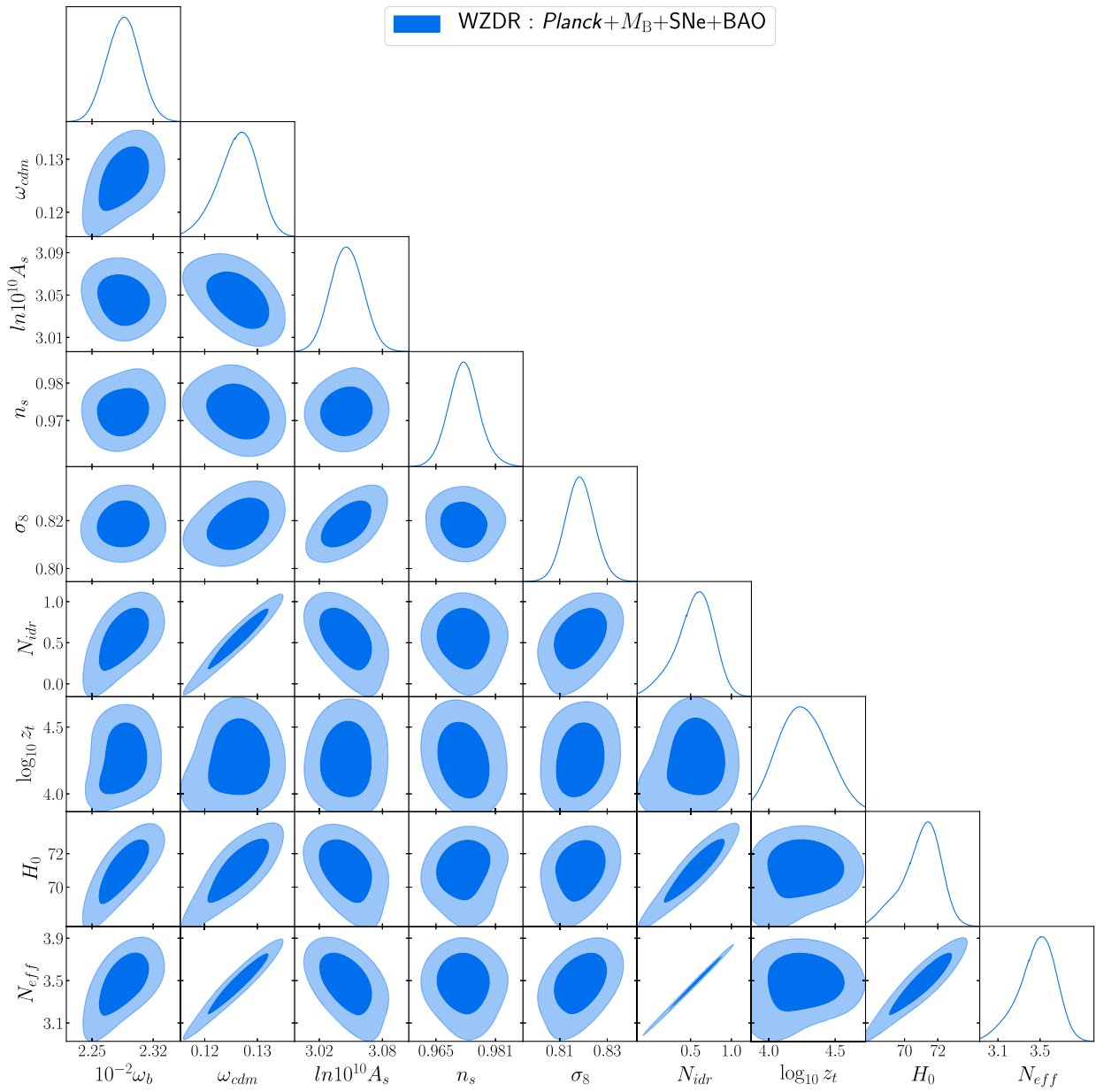


FIG. 7. Cosmological parameters constraints in WZDR model (with N_{wzdr} being the only extended parameter) from the datasets discussed in Appendix A.

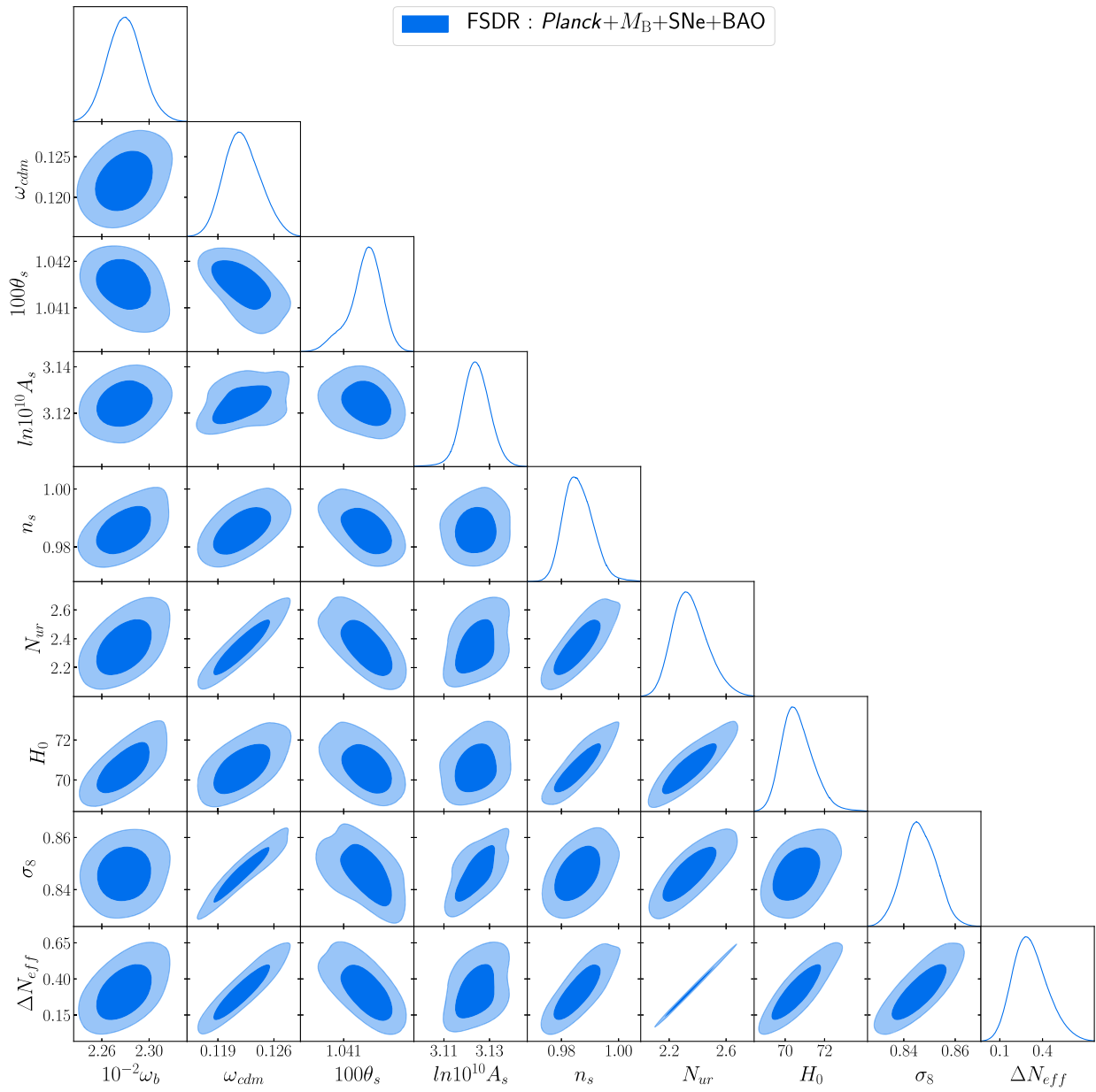


FIG. 8. Cosmological parameters constraints in FSDR model (with N_{ur} being a free parameter) from the datasets discussed in Appendix A.

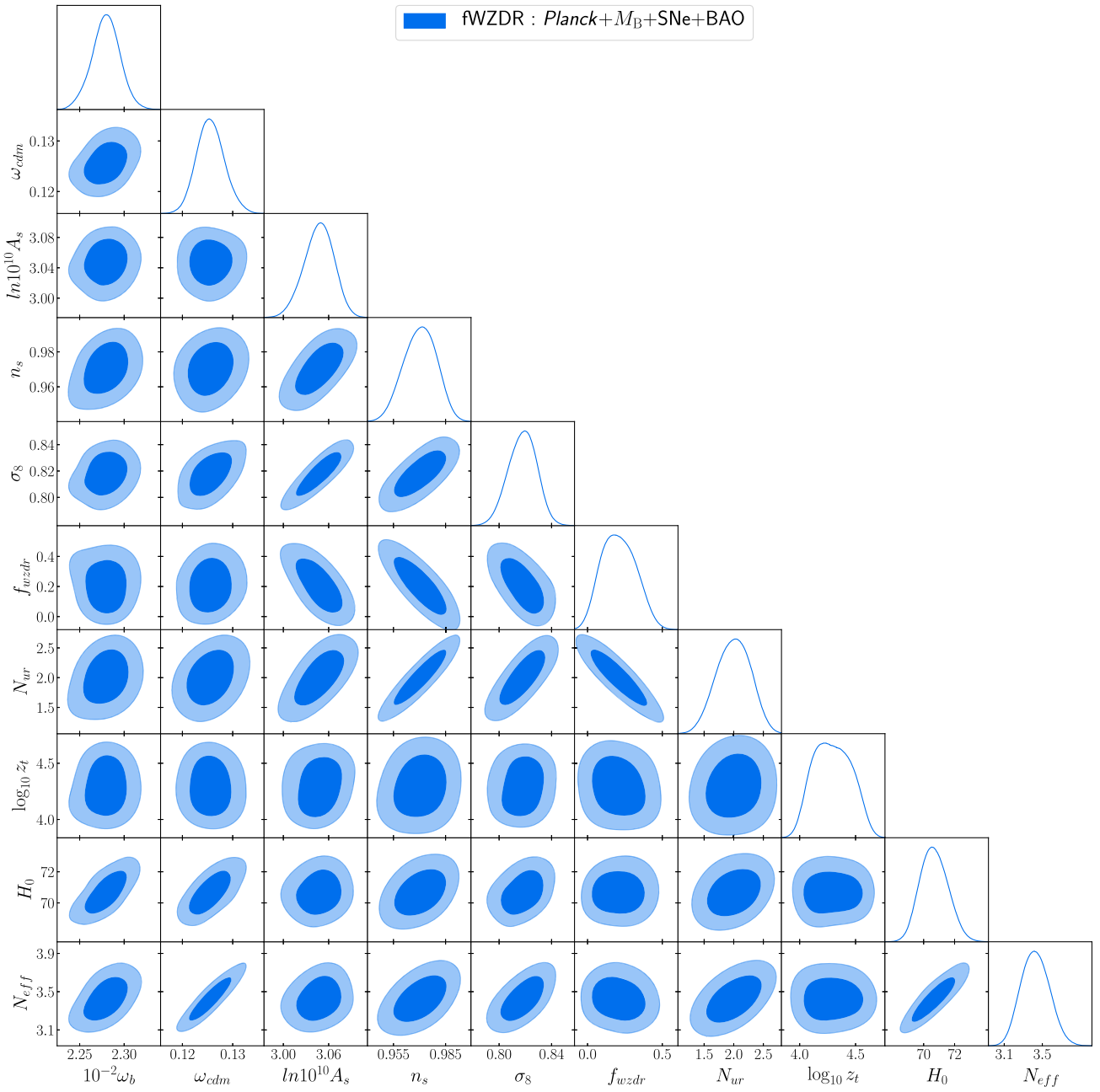


FIG. 9. Cosmological parameters constraints in (f)WZDR model (with f_{wzdr} and N_{ur} being free parameters) from the datasets discussed in Appendix A.

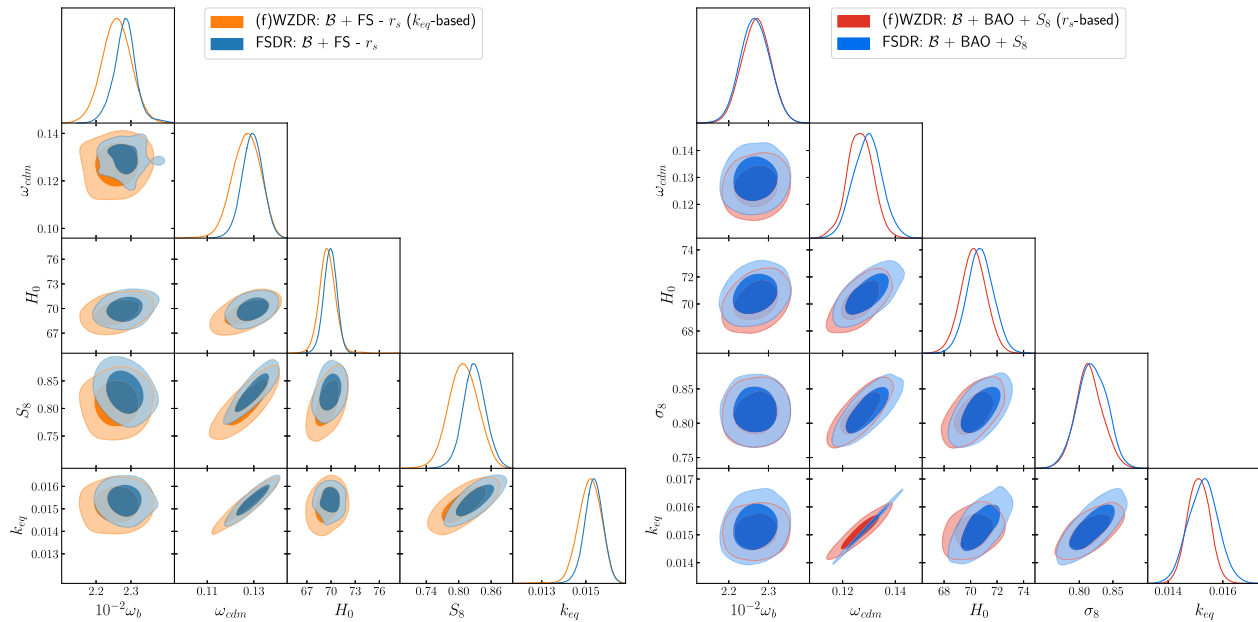


FIG. 10. Cosmological parameters constraints on WZDR model and FSDR model from k_{eq} -based datasets (left panel) and r_s -based datasets (right panel).

TABLE IV. The the mean $\pm 1\sigma$ constraints on the cosmological parameters and derived parameters in the WZDR and FSDR models from k_{eq} - and r_s -based datasets. Upper and lower bounds correspond to the 68% C.L. interval.

Dataset	k_{eq} -based		r_s -based	
	(f)WZDR	FSDR	(f)WZDR	FSDR
H_0	69.7 ± 1.1	$69.9^{+0.7}_{-0.6}$	70.2 ± 1.0	70.6 ± 1.0
$10^2 k_{eq}$	$1.517^{+0.055}_{-0.050}$	1.536 ± 0.038	1.512 ± 0.041	1.545 ± 0.021
σ_8	0.809 ± 0.027	$0.829^{+0.025}_{-0.029}$	0.815 ± 0.019	0.819 ± 0.022
Ω_m	$0.310^{+0.011}_{-0.0094}$	0.313 ± 0.09	0.304 ± 0.08	0.304 ± 0.08
χ^2_{\min}	1072.1	1072.8	7.8	8.3

- [1] A. G. Riess, S. Casertano, W. Yuan, J. B. Bowers, L. Macri, J. C. Zinn, and D. Scolnic, *Astrophys. J. Lett.* **908**, L6 (2021).
- [2] A. G. Riess *et al.*, *Astrophys. J. Lett.* **934**, L7 (2022).
- [3] T. Abbott *et al.* (DES Collaboration), *Phys. Rev. D* **98**, 043526 (2018).
- [4] S. Alam *et al.* (BOSS Collaboration), *Mon. Not. R. Astron. Soc.* **470**, 2617 (2017).
- [5] H. Hildebrandt *et al.*, *Astron. Astrophys.* **633**, A69 (2020).
- [6] C. Hikage *et al.* (HSC Collaboration), *Publ. Astron. Soc. Jpn.* **71**, 43 (2019).
- [7] E. Di Valentino, O. Mena, S. Pan, L. Visinelli, W. Yang, A. Melchiorri, D. F. Mota, A. G. Riess, and J. Silk, *Classical Quantum Gravity* **38**, 153001 (2021).
- [8] L. Perivolaropoulos and F. Skara, *New Astron. Rev.* **95**, 101659 (2022).
- [9] E. Abdalla *et al.*, *J. High Energy Astrophys.* **34**, 49 (2022).
- [10] W. L. Freedman, *Astrophys. J.* **919**, 16 (2021).
- [11] N. Aghanim *et al.* (Planck Collaboration), *Astron. Astrophys.* **641**, A6 (2020); **652**, C4(E) (2021).
- [12] L. Chen, Q.-G. Huang, and K. Wang, *J. Cosmol. Astropart. Phys.* **02** (2019) 028.
- [13] H. Gil-Marín *et al.*, *Mon. Not. R. Astron. Soc.* **477**, 1604 (2018).
- [14] J. E. Bautista *et al.*, *Astron. Astrophys.* **603**, A12 (2017).
- [15] E. Mortsell, A. Goobar, J. Johansson, and S. Dhawan, *Astrophys. J.* **933**, 212 (2022).
- [16] L. Perivolaropoulos, *Universe* **8**, 263 (2022).

- [17] L. Perivolaropoulos and F. Skara, *Phys. Rev. D* **104**, 123511 (2021).
- [18] G. Benevento, W. Hu, and M. Raveri, *Phys. Rev. D* **101**, 103517 (2020).
- [19] G. Alestas, D. Camarena, E. Di Valentino, L. Kazantzidis, V. Marra, S. Nesseris, and L. Perivolaropoulos, *Phys. Rev. D* **105**, 063538 (2022).
- [20] R. E. Keeley, S. Joudaki, M. Kaplinghat, and D. Kirkby, *J. Cosmol. Astropart. Phys.* **12** (2019) 035.
- [21] Z. Zhou, G. Liu, Y. Mu, and L. Xu, *Mon. Not. R. Astron. Soc.* **511**, 595 (2022).
- [22] G. Alestas, I. Antoniou, and L. Perivolaropoulos, *Universe* **7**, 366 (2021).
- [23] B. A. Bassett, M. Kunz, J. Silk, and C. Ungarelli, *Mon. Not. R. Astron. Soc.* **336**, 1217 (2002).
- [24] X. Li and A. Shafieloo, *Astrophys. J. Lett.* **883**, L3 (2019).
- [25] A. Hernández-Almada, G. Leon, J. Magaña, M. A. García-Aspeitia, and V. Motta, *Mon. Not. R. Astron. Soc.* **497**, 1590 (2020).
- [26] G. Efstathiou, *Mon. Not. R. Astron. Soc.* **505**, 3866 (2021).
- [27] S. Vagnozzi, *Phys. Rev. D* **104**, 063524 (2021).
- [28] R.-G. Cai, Z.-K. Guo, S.-J. Wang, W.-W. Yu, and Y. Zhou, *Phys. Rev. D* **106**, 063519 (2022).
- [29] J. L. Bernal, L. Verde, and A. G. Riess, *J. Cosmol. Astropart. Phys.* **10** (2016) 019.
- [30] V. Poulin, T. L. Smith, T. Karwal, and M. Kamionkowski, *Phys. Rev. Lett.* **122**, 221301 (2019).
- [31] T. L. Smith, V. Poulin, and M. A. Amin, *Phys. Rev. D* **101**, 063523 (2020).
- [32] A. Moss, E. Copeland, S. Bamford, and T. Clarke, *arXiv:2109.14848*.
- [33] K. V. Berghaus and T. Karwal, *Phys. Rev. D* **101**, 083537 (2020).
- [34] J. C. Hill and E. J. Baxter, *J. Cosmol. Astropart. Phys.* **08** (2018) 037.
- [35] R. Murgia, G. F. Abellán, and V. Poulin, *Phys. Rev. D* **103**, 063502 (2021).
- [36] S. Nojiri, S. D. Odintsov, and V. K. Oikonomou, *Phys. Dark Universe* **29**, 100602 (2020).
- [37] K. Rezazadeh, A. Ashoorioon, and D. Grin, *arXiv:2208.07631*.
- [38] S. Carneiro, P. C. de Holanda, C. Pigozzo, and F. Sobreira, *Phys. Rev. D* **100**, 023505 (2019).
- [39] L. Feng, R.-Y. Guo, J.-F. Zhang, and X. Zhang, *Phys. Lett. B* **827**, 136940 (2022).
- [40] G. Alestas, L. Kazantzidis, and L. Perivolaropoulos, *Phys. Rev. D* **103**, 083517 (2021).
- [41] V. Marra and L. Perivolaropoulos, *Phys. Rev. D* **104**, L021303 (2021).
- [42] K. L. Pandey, T. Karwal, and S. Das, *J. Cosmol. Astropart. Phys.* **07** (2020) 026.
- [43] N. Becker, D. C. Hooper, F. Kahlhoefer, J. Lesgourgues, and N. Schöneberg, *J. Cosmol. Astropart. Phys.* **02** (2021) 019.
- [44] H. Velten, I. Costa, and W. Zimdahl, *Phys. Rev. D* **104**, 063507 (2021).
- [45] D. Harvey, R. Massey, T. Kitching, A. Taylor, and E. Tittley, *Science* **347**, 1462 (2015).
- [46] R. Krall, F.-Y. Cyr-Racine, and C. Dvorkin, *J. Cosmol. Astropart. Phys.* **09** (2017) 003.
- [47] M. A. Buen-Abad, M. Schmaltz, J. Lesgourgues, and T. Brinckmann, *J. Cosmol. Astropart. Phys.* **01** (2018) 008.
- [48] Z. Pan, M. Kaplinghat, and L. Knox, *Phys. Rev. D* **97**, 103531 (2018).
- [49] M. Escudero, L. Lopez-Honorez, O. Mena, S. Palomares-Ruiz, and P. Villanueva-Domingo, *J. Cosmol. Astropart. Phys.* **06** (2018) 007.
- [50] S. D. Odintsov and V. K. Oikonomou, *Europhys. Lett.* **137**, 39001 (2022).
- [51] S. D. Odintsov and V. K. Oikonomou, *Europhys. Lett.* **139**, 59003 (2022).
- [52] S. Nojiri, S. D. Odintsov, and V. K. Oikonomou, *Nucl. Phys. B* **980**, 115850 (2022).
- [53] C. Krishnan, E. O. Colgáin, M. M. Sheikh-Jabbari, and T. Yang, *Phys. Rev. D* **103**, 103509 (2021).
- [54] J. C. Hill, E. McDonough, M. W. Toomey, and S. Alexander, *Phys. Rev. D* **102**, 043507 (2020).
- [55] V. Poulin, T. L. Smith, D. Grin, T. Karwal, and M. Kamionkowski, *Phys. Rev. D* **98**, 083525 (2018).
- [56] A. Gogoi, R. K. Sharma, P. Chanda, and S. Das, *Astrophys. J.* **915**, 132 (2021).
- [57] T. L. Smith, M. Lucca, V. Poulin, G. F. Abellan, L. Balkenhol, K. Benabed, S. Galli, and R. Murgia, *Phys. Rev. D* **106**, 043526 (2022).
- [58] D. Aloni, A. Berlin, M. Joseph, M. Schmaltz, and N. Weiner, *Phys. Rev. D* **105**, 123516 (2022).
- [59] O. Seto and Y. Toda, *Phys. Rev. D* **103**, 123501 (2021).
- [60] C. Dvorkin, M. Wyman, D. H. Rudd, and W. Hu, *Phys. Rev. D* **90**, 083503 (2014).
- [61] A. Aboubrahim, M. Klasen, and P. Nath, *J. Cosmol. Astropart. Phys.* **04** (2022) 042.
- [62] G. Steigman, *Phys. Rev. D* **87**, 103517 (2013).
- [63] S. Ghosh, S. Kumar, and Y. Tsai, *J. Cosmol. Astropart. Phys.* **05** (2022) 014.
- [64] S. Vagnozzi, *Phys. Rev. D* **102**, 023518 (2020).
- [65] K. Jedamzik, L. Pogosian, and G.-B. Zhao, *Commun. Phys.* **4**, 123 (2021).
- [66] C. Krishnan, E. O. Colgáin, Ruchika, A. A. Sen, M. M. Sheikh-Jabbari, and T. Yang, *Phys. Rev. D* **102**, 103525 (2020).
- [67] E. O. Colgáin, M. M. Sheikh-Jabbari, R. Solomon, G. Bargiacchi, S. Capozziello, M. G. Dainotti, and D. Stojkovic, *Phys. Rev. D* **106**, L041301 (2022).
- [68] E. O. Colgáin, M. M. Sheikh-Jabbari, R. Solomon, M. G. Dainotti, and D. Stojkovic, *arXiv:2206.11447*.
- [69] K. C. Wong *et al.*, *Mon. Not. R. Astron. Soc.* **498**, 1420 (2020).
- [70] G. D'Amico, L. Senatore, P. Zhang, and H. Zheng, *J. Cosmol. Astropart. Phys.* **05** (2021) 072.
- [71] O. H. E. Philcox, B. D. Sherwin, G. S. Farren, and E. J. Baxter, *Phys. Rev. D* **103**, 023538 (2021).
- [72] G. S. Farren, O. H. E. Philcox, and B. D. Sherwin, *Phys. Rev. D* **105**, 063503 (2022).
- [73] E. J. Baxter and B. D. Sherwin, *Mon. Not. R. Astron. Soc.* **501**, 1823 (2021).
- [74] O. H. E. Philcox, G. S. Farren, B. D. Sherwin, E. J. Baxter, and D. J. Brout, *Phys. Rev. D* **106**, 063530 (2022).
- [75] D. Brout *et al.*, *Astrophys. J.* **938**, 110 (2022).
- [76] J. Wess and B. Zumino, *Nucl. Phys.* **B70**, 39 (1974).

- [77] F. Beutler *et al.* (BOSS Collaboration), *Mon. Not. R. Astron. Soc.* **464**, 3409 (2017).
- [78] S. Alam *et al.* (SDSS-III Collaboration), *Astrophys. J. Suppl. Ser.* **219**, 12 (2015).
- [79] K. S. Dawson *et al.* (BOSS Collaboration), *Astron. J.* **145**, 10 (2013).
- [80] A. Chudaykin, M. M. Ivanov, O. H. E. Philcox, and M. Simonović, *Phys. Rev. D* **102**, 063533 (2020).
- [81] M. M. Ivanov, M. Simonović, and M. Zaldarriaga, *J. Cosmol. Astropart. Phys.* **05** (2020) 042.
- [82] E. van Uitert *et al.*, *Mon. Not. R. Astron. Soc.* **476**, 4662 (2018).
- [83] T. Hamana *et al.*, *Publ. Astron. Soc. Jpn.* **72**, 16 (2020).
- [84] J. Lesgourgues, [arXiv:1104.2932](https://arxiv.org/abs/1104.2932).
- [85] D. Blas, J. Lesgourgues, and T. Tram, *J. Cosmol. Astropart. Phys.* **07** (2011) 034.
- [86] A. Mead, J. Peacock, C. Heymans, S. Joudaki, and A. Heavens, *Mon. Not. R. Astron. Soc.* **454**, 1958 (2015).
- [87] A. Mead, *Mon. Not. R. Astron. Soc.* **464**, 1282 (2017).
- [88] A. Mead, S. Brieden, T. Tröster, and C. Heymans, *Mon. Not. R. Astron. Soc.* **502**, 1401 (2020).
- [89] T. Brinckmann and J. Lesgourgues, *Phys. Dark Universe* **24**, 100260 (2019).
- [90] N. Schöneberg, G. Franco Abellán, A. Pérez Sánchez, S. J. Witte, V. Poulin, and J. Lesgourgues, *Phys. Rep.* **984**, 1 (2022).
- [91] N. Aghanim *et al.* (Planck Collaboration), *Astron. Astrophys.* **641**, A5 (2020).
- [92] F. Beutler, C. Blake, M. Colless, D. H. Jones, L. Staveley-Smith, L. Campbell, Q. Parker, W. Saunders, and F. Watson, *Mon. Not. R. Astron. Soc.* **416**, 3017 (2011).
- [93] A. J. Ross, L. Samushia, C. Howlett, W. J. Percival, A. Burden, and M. Manera, *Mon. Not. R. Astron. Soc.* **449**, 835 (2015).
- [94] D. M. Scolnic *et al.*, *Astrophys. J.* **859**, 101 (2018).
- [95] D. Camarena and V. Marra, *Mon. Not. R. Astron. Soc.* **504**, 5164 (2021).